High Reynolds Number Helicopter Fuselage Test in the ONERA F1 Pressurised Wind Tunnel

J. Gatard (ONERA) and M. Costes (ONERA), N. Kroll (DLR), P. Renzoni (CIRA),
A. Kokkalis (GKN - WHL), A. Rocchetto (AGUSTA), C. Serr (ECF),
E. Larrey (SIMULOG), A. Filippone (DTU), D. Wehr (IAG)

Abstract

The objective of the joint European HELIFUSE research project is to improve the helicopter fuselage drag reduction capabilities of the European rotorcraft industry, by obtaining a better understanding of the helicopter fuselage flow field and the subsequent improvement of aerodynamic design codes.

Within the framework of this project, a wind tunnel test programme was performed to procure a complete database of fuselage forces and moments, surface pressures and surface flow visualisation on a realistic modular fuselage, including data on simpler fuselage shapes well-suited for preliminary design code validation, at various Reynolds numbers.

The data obtained is also to be used for an investigation into the influence of Reynolds number variation upon the magnitude of the forces and moments acting upon the fuselage.

The test programme was conducted in the F1 pressurised low speed wind tunnel of Le Fauga-Mauzac ONERA Centre, utilising the 1/4-scale DGV200 fuselage model of the EUROCOPTER "Dauphin à Grande Vitesse" helicopter.

Several different measurement techniques were used during these tests.

These were:

- surface pressure measurements (up to 200 pressure taps) with multi transducer modules,
- aerodynamic loads measurements using a six component balance,
- coloured oil flow separation and skin-friction lines visualisation,
- acenaphtene sublimation for transition line visualisation,
- hot films for the determination of the position of the transition line

The quality of the measured data was continuously monitored to achieve the best possible accuracy.

Notations

ALPHA, α	angle of attack (°)
BETA, β	sideslip angle (°)
Cx	drag coefficient
Conf	configuration
Kp	pressure coefficient
M0	reference Mach number
PI0	stagnation pressure (Pa)
Q0	dynamic pressure (Pa)
RE0	reference Reynolds number calculated with the full rotor diameter
rms	root mean square value

1. Introduction

The fuselage is one of the major sources of drag for the helicopter in forward flight conditions. At high speed, about 50% of the power delivered by the main rotor is used to counterbalance the aerodynamic forces acting on the fuselage. Consequently,

evaluation and reduction of the helicopter fuselage drag (HFD) is of primary interest to the rotorcraft industry because of its adverse effects upon the helicopter's speed, range and capability, and thus overall operational costs. It is of no surprise therefore that fuselage drag reduction, and thus increased helicopter efficiency, has been identified by the European helicopter manufacturers as one of the key issues to address in their desire to expand the helicopter market during the next century.

To achieve a significant HFD reduction from the early stages of the design process, for example by fuselage shape optimisation, reliable prediction tools [1 to 4] have to be developed, and which are supported by high quality wind tunnel test data.

The present state-of-the-art in terms of helicopter fuselage numerical simulation and optimisation, is far from what industry requires. Most of the existing design tools are based on inviscid panel methods, sometimes coupled to boundary layer codes. Due to the geometrical complexity of the fuselage, especially around the rotor hub and fairing, the flow around it is strongly dependant on viscous effects, with flow separation occurring downstream of the rotor hub. Thus, such codes have significant limitations in their capability to correctly predict the resultant forces and moments, particularly the drag, to the accuracy required for design purposes.

More recently, Navier-Stokes calculations have been conducted on simple generic fuselage shapes, but have still to be applied on realistic fuselage bodies [5 to 7]. This is partly due to the difficulty in generating well-adapted grids on such complex configurations, and partly to the turbulence modelling requirements for these highly three-dimensional flows.

Thus, as a result of the theoretical model limitations, fuselage shape design is still entirely based on wind tunnel tests of small scale models [8]. Such tests, however, are conducted at significantly lower Reynolds numbers to those encountered at flight conditions, implying that extrapolations have to be made when estimating the overall helicopter performance at full scale flight Reynolds number. For these extrapolations to be accurate they generally require that some full-scale data from an existing helicopter shape that is close enough to the new design is already available to the designer. Even when such data is available, which is not always the case, this design methodology may lead to erroneous predictions and eventually the wrong design, thus significantly increasing the product development time and cost.

In order to overcome these limitations, a comprehensive research activity was set up by the partners of the HELIFUSE EC-co-funded BRITE/EURAM Programme, which includes both the numerical computations and wind tunnel testing of a modular helicopter fuselage at various Reynolds numbers.

The HELIFUSE wind tunnel tests were conducted in September 1996 in the F1 pressurised wind tunnel. The primary aim of the tests was to construct a comprehensive data base of surface pressures and overall forces and moments acting upon different fuselage shapes over a range of Reynolds numbers up to full scale one. For the purpose of design code validation, data on simpler fuselage shapes which are particularly well-suited for validation of advanced CFD codes, was thus obtained. A secondary aim of the tests was to experimentally investigate the influence due to Reynolds number variation on the magnitude of the forces and moments acting upon the fuselage.

A parallel effort is currently being made with computational methods by adapting Navier-Stokes algorithms to low-speed conditions. This work would allow comparisons, using similar grids, to be made of the drag prediction capabilities of the various adapted algorithms with test data.

The present paper will mainly describe the experimental aspects of this co-operative project and show typical results, including comparisons with boundary layer calculations and preliminary CFD computations where available.

2. The F1 pressurised wind tunnel

The F1 pressurised wind tunnel is a low speed, high Reynolds number wind tunnel which has been designed for high productivity, preserving test quality and confidentiality.

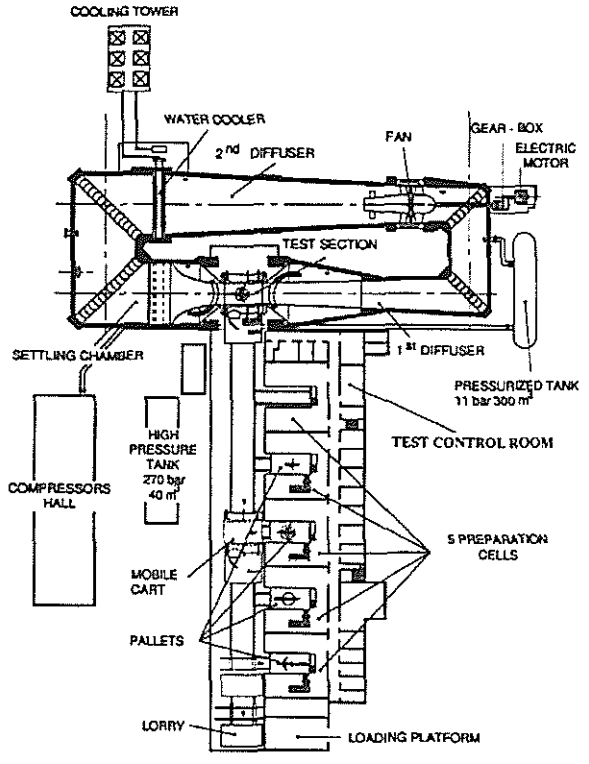

Fig. 1 : The F1 wind tunnel

It is a continuously operating close circuit wind tunnel (180 m overall length). Most of the circuit shell consists of epoxy resin coated prestressed concrete, to support the 3.85 bar maximum stagnation pressure. Contraction fan shroud and test section envelope are made of steel.

The rectangular shape guided test section is 11m long by 4.5 m wide by 3.5 m high. The walls and ceiling are made of plywood, supporting lighting and control windows. The test section and its pressurised cylindrical envelope are movable and can receive one of the four pallets constituting the test section floor. Each pallet includes the model support and a dedicated data acquisition unit, enabling the complete test preparation in the isolated cells.

The 16 blades variable-pitch constant-speed fan (7.4 m in diameter, with 3.8 m diameter hub) is driven by a 9.5 MW electric motor, mounted outside the wind tunnel. The Mach number is adjusted by changing the blades pitch angle. A 17 blade diffuser supports the fan tail cone. An automated water cooler regulates the wind tunnel temperature.

A 200 mm thick honeycomb, followed by three fine mesh grids, located upstream of the convergence, ensures a low turbulence level in the test section.

Since its opening, great emphasis has been placed upon the productivity and versatility of the F1 wind tunnel. These have been addressed by the

- complete test preparation on the pallet outside the wind tunnel circuit, including all instrumentation testing,
- gate valves concept allowing quick access to the model (about 10 minutes) or pallet exchange while the circuit is pressurised (about 1 hour).
- variable pitch propeller allowing quick wind tunnel speed variations (1 minute from 0 up to the maximum)
- automatically driven compressor unit which can pressurise the whole tunnel from 1 to 3.85 bar in less than one and a half hour.

3. The DGV200 model

The DGV200 model is a 1/4th scale fuselage model of the EUROCOPTER "Dauphin à Grande Vitesse" helicopter. It has been manufactured by ONERA's "Institut de Mécanique des Fluides de Lille".

This model is made of a central steel structure, completed by composite elements. The modular design of the model the following four configurations to be tested :

- C1 : basic fuselage,
- C2 : C1 + engine fairing,
- C3 : C2 + rotor,
- C4 : C3 + rear parts.

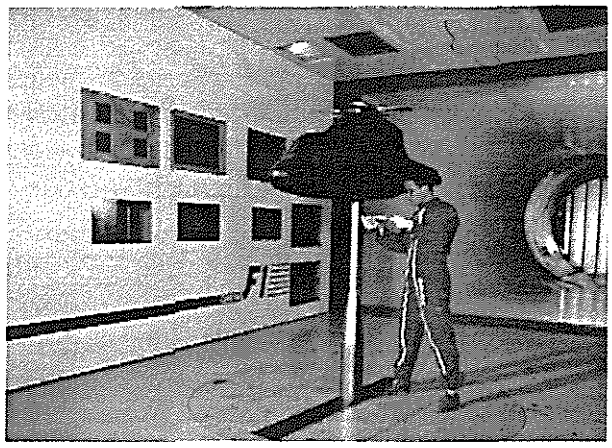

Fig. 2 : DGV200 model, C3 configuration in the F1 wind tunnel test section.

The fuselage is made of a central steel box receiving the balance supporting sting. The plane faces of the box are covered with composite fairing representing the exact form of the real helicopter. Its upper part can be fitted, either with a simplified fairing (C1 configuration) or with the engine fairing, with or without the rotor electrical motor inside. The instrumentation (inclinometers, PSI multi transducers, pressure probes...) is placed in a fore box.

The five-bladed rotor is represented by its blade roots extending up to the first aerofoil section of the blades. The blade root pitch angle can be set at any prescribed value by a mechanical device. For the present tests, a 20° pitch angle was selected, corresponding to a typical high-speed flight value. This reduced rotor has a diameter of 775 mm, with the rotor shaft angle pitched 4° forward, with respect to the fuselage axis. The rotor fairing can be replaced by a closed fairing when no rotor equips the model (C2 configuration).

The rotor is motorised by a 3 kW asynchronous electrical motor through a 1/3 reduction gear. The electric power is fed via a rheostatic switch. The motor is cooled by a continuous circulation of water. The motor speed is measured by a magnetic sensor mounted on the motor's main shaft. Careful installation ensures that the power line does not produce EMC interference to the pressure and force signal wires.

During the present tests, only the C1, C2 and C3 fuselage configurations were tested.

4. Measuring means

The experimental set-up used in this wind tunnel test programme is shown in Figure 3 and comprises of :

- a 2m diameter turntable, providing the azimuth (BETA) angle, upon which is mounted the ALPHA table ;
- the ALPHA table, which allows a model pitch sweep between -17° and +17° ;
- the 80 mm strut, fitted with a streamlined fairing allowing the passage of the measurement wires, the motor's electrical power lines and the water cooling pipes. At its top is fixed a support plate with the balance attachment fitting ;
- the Φ120 six-component balance ;
- the DGV200 motorised model.

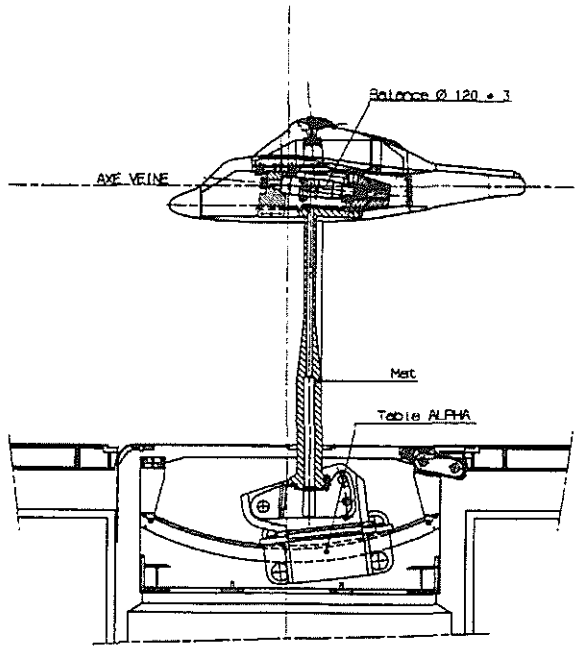

Fig. 3 : Experimental set-up

Pitch attitude is measured by two inclinometers fastened on a bracket. This bracket is bolted to the central steel box upper face. For this test, the pitch attitude measurement equipment were calibrated over the range from - 6,5° to + 6,5°. The angular reference is given by a bubble inclinometer, resting on a bracket bolted on the upper front part of the fuselage, parallel to the fuselage longitudinal axis. An electrical pre-set zero degree indicator allows more rapid positioning at 0° during the tests.

Azimuth angle is measured by the encoder and the potentiometer which equip the turntable. The zero angle is given by alignment of the model longitudinal axis with the wind tunnel longitudinal axis. For this test, the potentiometer was calibrated from -6° to +6°.

A 120 mm diameter balance is used to measure the global forces and moments on the model. It is a six strain gauges bridges - six component balance. The capability of the balance, along the respective axis of each load component, is as follows :

• drag	±	3 800	N
• side force	±	29 800	N
• lift	±	55 400	N
• rolling moment	±	6 400	N.m
• yawing moment	±	6 300	N.m
• pitching moment	±	2 650	N.m

To increase balance capability on lateral loads measurement, this balance was rotated by +90° around the spin axis.

The limit stresses are monitored by a dedicated balance control software which continuously calculates the internal loads in the balance. An indication of these loads is displayed in the control room. The loads experienced by the balance during the tests never exceeded the safety limits. Finally, a contact detector is set between the strut and the outer shell of the model in order to avoid wrong measurements due to unexpected contact interference. The output from this contact detector is also displayed in the control room during the tests.

The pressure measurement system uses an airtight tank to generate the back-pressure for the PSI modules, allowing the use of differential transducers in order to increase the measurement accuracy. The fuselage model is fitted with 231 static pressure taps, arranged in 26 measurement sections. Depending on the configuration, 188 to 207 taps can be used simultaneously. Six PSI modules of ± 5 psi range (± 35000 Pa) group all the taps, but of these only five are used simultaneously, since the engine fairing taps (C2 and C3 configurations) and flat fairing taps (C1 configuration) are routed to two separated modules. Figure 4 shows the pressure taps distribution for the C1 and C2 configurations.

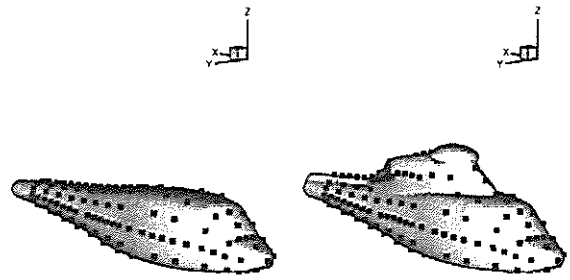

Fig. 4 : Pressure taps position on C1 and C2 configurations

For the pressure and loads measurements, after setting stable conditions in terms of stagnation pressure, Mach number and model attitude, a set of 30 points (called a lot) is recorded, at a 1 Hz rate.

The data reduction is initially done in real time on a slave computer which allows for real time editions and monitoring, and then by the main computer for off-line processing and storage of results. The two data reduction steps (i.e. real and off- line) use the same software to convert the acquired signals into physical values and then to postprocess these values (various corrections, coefficients calculations, Kp,...).

The final results are written and stored in the output file. The wall corrected coefficients are plotted point by point in real time during the tests. After the end of each loads measurement lot (30 points), an histogram of the drag coefficient variation is plotted to check the stability of the measurement conditions

In order to determine the position of the transition on the model at various conditions (Reynolds number, angle of attack, Mach number, ...) acenaphtene sublimation visualisation is used.

The model is sprayed with a white mixture of acetone and naphthalene. The skin friction coefficient is higher in a turbulent boundary layer than in a laminar boundary layer. This effect causes the mixture to sublimate, once

the desired test condition is established, resulting in a colour change on the fuselage surface (see figure 14).

After running a test configuration, the wind tunnel is opened and photographs are taken from defined points, to be compared with reference shots taken from the same points. During the run, a video tape is also recorded, which allows for the evolution of the visualisation to be captured.

To visualise the skin friction lines on the model, a mixture of oil and pigments is used to paint the model after protecting the pressure taps. Once the test conditions are achieved, the oil flows, following the skin friction lines. The same recording procedure as for the acenaphtene visualisation is then used to capture the flow evolution.

Figure 5 shows an example of a photo taken after an oil flow visualisation run for the C2 configuration.

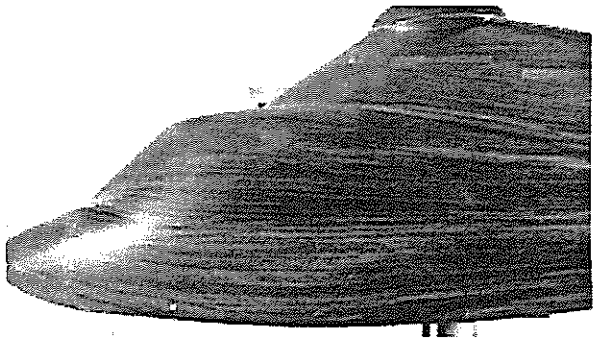

Fig. 5 : Oil flow visualisation, C2 configuration, RE0 = 30 million

Hot films were also used (32 in total), to assess the position of the transition zone on both sides and below the nose of the fuselage model. Figure 6 shows the positions of the hot films on the fuselage. Transition locations are obtained by the examination of the time-dependant instantaneous hot films signals and X-dependant rms signals. In a laminar boundary layer the signals are not disturbed whereas when transition occurs, turbulent spots are visible and rms values suddenly increase. In a turbulent boundary layer, the rms levels remain fairly constant but are higher than those for the laminar boundary layer.

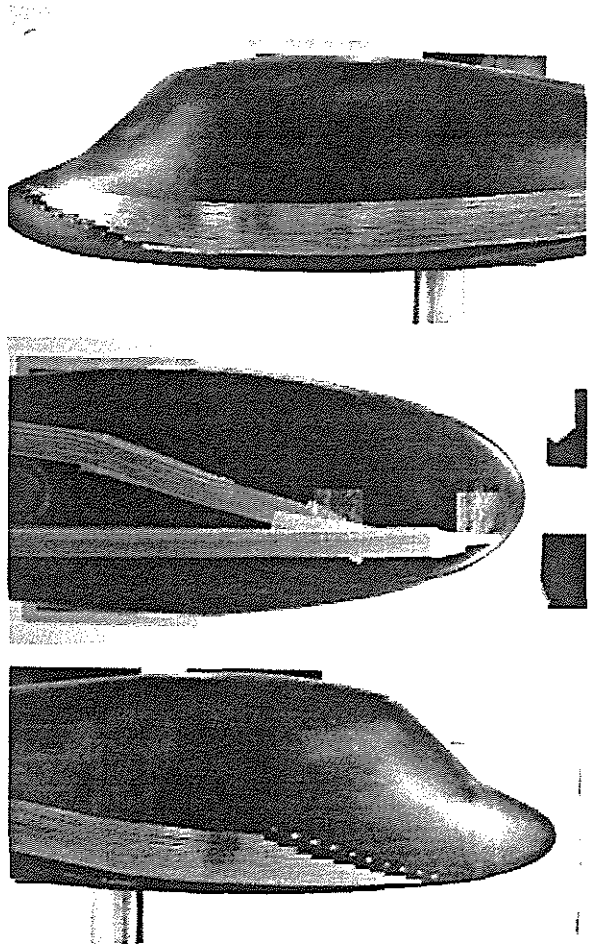

Fig. 6 : Hot films position on the fuselage

5. Test programme

The objective of this wind tunnel test was twofold :

- to obtain a well-documented database suitable for the validation of Navier-Stokes methods,
- to investigate the effect of Reynolds number variation on the magnitude of the forces and moments acting upon the fuselage.

The first objective was well attained by the use of a modular fuselage model, which allowed the investigation of both simple as well as more complex, realistic fuselage configurations. The second objective was also satisfied by the capability of the F1 wind tunnel to vary the stagnation pressure and Mach number independently to each other.

The wind tunnel tests took place during a one week entry in F1 during fall 1996. As indicated above, only the C1, C2 and C3 configurations were tested. The test

programme included more than 72 test points for pressure and loads measurements, and 11 test points for flow visualisation (acenaphtene and oil-flow) and hot-films measurements.

The test conditions covered three incidence values (-5°, 0° and +5°) and three values for the sideslip angle (-6°, 0° and +6°). By varying the stagnation pressure from 1 to 3.85 bar and the wind tunnel velocity from 30 to 80 m/s, the Reynolds number could be varied from 6 million up to 60 million.

The lower bound corresponds to a typical value at which standard wind tunnel models are currently tested during the design process. The upper bound corresponds to the actual flight Reynolds number. Flow visualisations and the hot-films measurements, which are more time-consuming, were completed only for a limited number of configuration.

In particular, the emphasis for these tests was placed upon the five configurations selected by the Partners for their Navier-Stokes blind-test calculations so that data availability for CFD code validation was maximised.

It should be also mentioned at this point that for safety reasons, the balance load limitations were chosen to be above the highest loads that might be encountered at the highest Reynolds number test points. This meant that for the loads and moments measured at the lowest Reynolds number test points, the balance resolution was not optimal.

In order to estimate the measurement dispersion due to this limitation, a statistical analysis of the 30 point samples was completed after each measurement condition.

6. Results

Some typical results for each type of measurement completed are shown hereafter. Also, whenever possible, comparisons with typical prediction calculations are presented to illustrate the two complementary activities of the HELIFUSE research programme.

6.1. Accuracy

For the tunnel references, static pressure is measured with 6 static pressure taps, which show a good agreement : the differences between them are of the order of a few dozen of Pascal. The corresponding relative errors on pressure coefficients are in the order of 0.3 % at PI0 = 3.85 bar, M0 = 0.235, and are even lower for reduced PI0 and M0 values.

The angle of attack is measured simultaneously by two inclinometers. The difference between the two measured values is about 1/100th of a degree. The sideslip angle is obtained from the turntable potentiometer indications, which is estimated accurate to about 3/100th of a degree.

For the loads and moments, the accuracy is estimated from the dispersion of the 30 points samples. It has to be calculated for the two extreme flow cases :

- Q0 of 14000 Pa (corresponding for example to PI0 = 3,85 bar and M0 = 0,233)
- Q0 of 540 Pa (corresponding for example to PI0 = 1 bar and M0 = 0,089)

Using a 3σ confidence interval for the measured values, the relative precision calculated for the two extreme flow cases is in the order of 0,1% of the balance capacity. Figure 7 shows an example of histogram obtained from this statistical analysis with a low Q0 case.

The results are presented in reduced variables (centred on the mean and normalised by the standard deviation) for the drag. Although the number of samples is relatively small, it can be seen that the scatter of the measured drag is well within the 3σ interval and therefore acceptable.

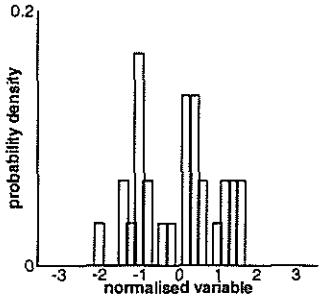

Fig. 7 : Example of statistical distribution for the drag at low Q0

6.2. Analysis of Results

In this section, some typical results from this wind tunnel test programme are shown, together with some comparisons with computed data when available.

The influence of the Reynolds number variation upon the fuselage drag values for the basic fuselage shape C1 is shown in figure 8. As expected, the influence of Reynolds number variation upon the measured drag values is most noticeable at the lower values of Reynolds number. For Reynolds number values above 30 million, the measured drag coefficient is almost constant. The slight increase at the highest Reynolds numbers is thought to be due to boundary layer separation on the aft part of the fuselage.

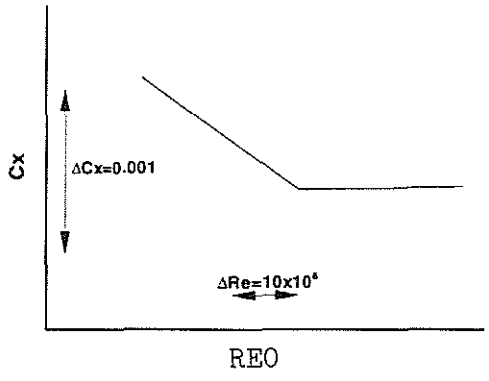

Fig. 8 : Influence of Reynolds number on drag coefficient

This Reynolds number effect, however, is not simple and strongly depends on the flight configuration. For example, figure 9 shows the influence of Reynolds number for the C2 configuration at several α and β. As it can be seen, the Reynolds number effect is maximum when the configuration is a zero incidence and sideslip angle, while, for β = - 6°, the drag slightly decreases at the lower Reynolds numbers. Such complex behaviour makes extrapolations from low Reynolds to flight Reynolds numbers more difficult.

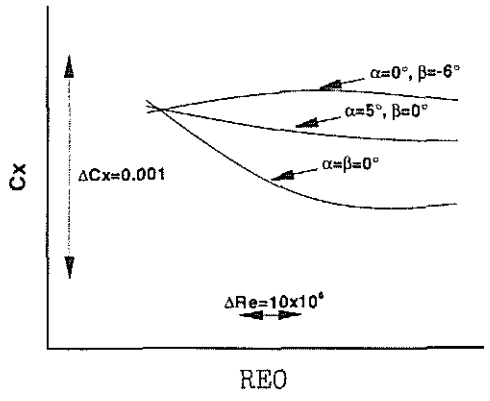

Fig. 9 : Influence off flight configuration on Reynolds number effect

The drag increment measured between configuration C1 (without any engine fairing), configuration C2 (with engine fairing) and configuration C3 (with the rotating blade roots), is given in figure 10. As it can be seen, the drag increment between the three configurations is considerable with the rotating blade roots having the most dramatic influence upon the level of the measured drag.

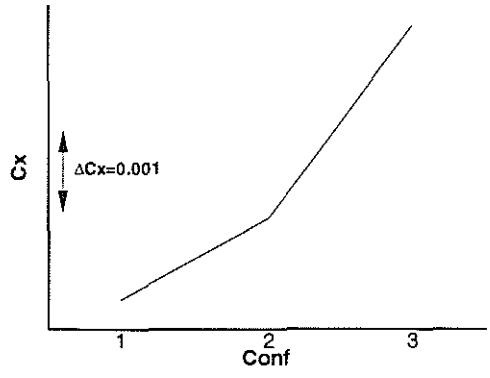

Fig. 10 : Influence of configuration on drag coefficient

The surface pressure distribution for the C1 configuration is shown on figure 11 and that for the C2 configuration is given in figure 12, both taken at a Reynolds number of 30 million.

Also shown for comparison are the data from a fully turbulent Navier-Stokes calculation. For these plots, the measured pressure was interpolated from the pressure tap's position onto the surface grid generated for use by the Navier-Stokes code.

As it may be observed, see figures 11 & 12, a fairly good correlation between the computed and the measured pressures is found, although the relatively limited number of pressure taps introduces some interpolation errors in the test data plotted.

For example, in the region around the nose of the fuselage the extend of the stagnation point is magnified whilst for some parts of the fuselage where there are no pressure taps the errors due to the data extrapolation are very apparent. This is particularly true for the rotor hub region of the C2 configuration.

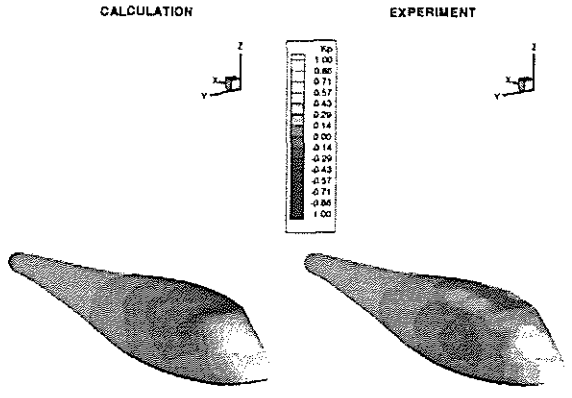

Fig. 11 : Comparison calculation-experiment for the pressure distribution (C1 configuration)

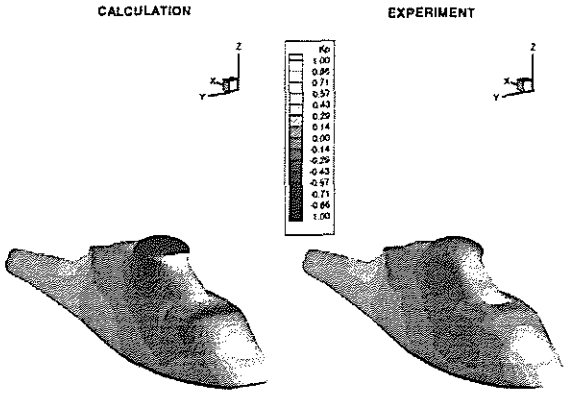

Fig. 12 : Comparison calculation-experiment for the pressure distribution (C2 configuration)

An example of the agreement obtained between the calculated and experimental pressure coefficient, Kp, on the fuselage centreline for the C2 configuration, is shown on figure 13.

This figure clearly shows the error present on the plotted experimental Kp due to the extrapolation used, in particular at the rotor hub and which was first noticed in figure 12. Furthermore, the sting supporting the model induces small local perturbations in the Kp values along the lower centreline of the fuselage that. Such perturbations are not present on the Navier-Stokes calculations and thus the agreement between the two data sets is not good in this area.

For the remaining parts of the fuselage centreline, however, the correlation between calculation and experiment is quite satisfactory.

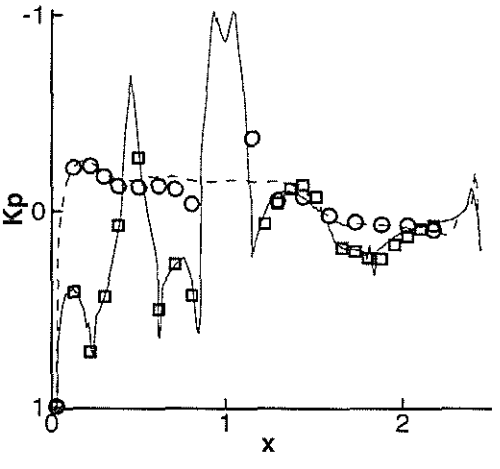

Fig. 13 : Kp calculation-experiment comparison for on the fuselage centreline

A comparison of the transition position between the wind tunnel acenaphtene visualisation and a boundary-layer calculation [9] at a Reynolds number of 30 million is given in figure 14. It is observed that transition appears fairly early for the top and the bottom of the fuselage nose, while a larger extend of laminar flow is found on the lateral surface of the fuselage. It is thought that the transition on the upper side is initiated by the strong adverse pressure

gradients occurring at the canopy, while on the lower side, the transition is probably due to the fuselage edge. It is also be seen that the complex three-dimensional shape of the transition line is well computed by the boundary layer analysis.

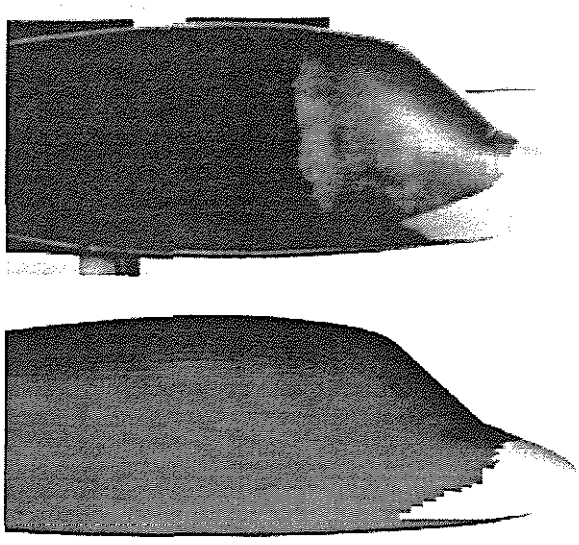

Fig. 14 Comparison of measured and computed transition position for the C1 configuration

7. Conclusions

This paper gives a brief description of the HELIFUSE European research programme tests in the F1 pressurised wind tunnel of the 1/4th scaled DGV200 helicopter fuselage model.

The objectives of the tests were to construct a comprehensive database of surface pressures and overall forces and moments acting upon different fuselage models over a range of Reynolds numbers up to full scale and to experimentally investigate the influence of the Reynolds number variation on the magnitude of the forces and moments acting upon the fuselage.

Both of the above test objectives were satisfactorily achieved, showing that the F1 pressurised wind tunnel is well suited for such studies. A preliminary analysis of the test data shows that the accuracy of the results is within the expected range. The results obtained also confirmed the complexity of the helicopter fuselage's flow field and the non-linear Reynolds number influence upon the magnitude of the force and moments coefficients. Further analysis of the database is still necessary, however, before the Partners obtain sufficient information which would allow them to extrapolate low-Reynolds number wind tunnel measurements to that of the full size rotorcraft with a high degree of accuracy. Finally, this high quality database will be very useful for the improvement and validation of Navier-Stokes CFD codes. This task is already underway within the HELIFUSE co-operation. Preliminary comparisons between blind-test CFD calculations and experimental data have already shown the great value of this database for such code evaluation and improvement.

Acknowledgements

This activity is partly funded by the European Union within the Area 3A Aeronautics of the Industrial an Materials Technologies Programme (BRITE/EURAM III).

References

[1] A.M. Vuillot, V. Couailler, N. Liamis "Three-dimensional Turbomachinery Euler and Navier-Stokes Calculations with a Multidomain Cell-centered Approach", 29th AIAA/ASME/ASEE Joint Propusion Conference and Exhibit, Monterey, 1993

[2] N.Kroll, N. Radespiel, C.C. Rossow "Accurate and Efficient Flow Solvers for 3D Applications on Structures Meshes", VKI CFD Lecture Series, Brussels, 1994

[3] M. Amato, A. Matrone, L. Paparono, P. Schiano "A Parallel 3D Multiblock Euler/Thin-Layer Navier-Stokes Flow Solver", Parallel CFD 94, Kyoto, 1994

[4] J.N. Sorensen "3D Navier-Stokes Method for Direct Simulation of Vortex Breakdown", Vieweg Notes on Numerical Fluid Mechanics, 42, 109-110

[5] J.C. Narramore. "Navier-Stokes computation of fuselage drag increments", AHS Aeromechanics Specialists Conference, San Francisco, January 19-21, 1994.

[6] E.P.N. Duque, A.C.B. Dimanlig, "Navier-Stokes simulation of the AH-66 Comanche Helicopter", AHS Aeromechanics Specialists Conference, San Francisco, January 19-21, 1994.

[7] J.D. Berry, M.S. Chaffin, E.P.N. Duque, "Helicopter fuselage aerodynamic predictions : Navier-Stokes and Panel Method solutions and comparison with experiment", AHS Aeromechanics Specialists Conference, San Francisco, January 19-21, 1994

[8] A. Cler "High-Speed Dauphin Fuselage Aerodynamics", 15th European Rotorcraft Forum, Amsterdam, 1989

[9] R. Houdeville "Three-Dimensional Boundary Layer Calculation by a Characteristic Method", 5th Symposium on Numerical and Physical Aspects of Aerodynamic Flows, Long Beach, 1992.